IEEE Access
Multidisciplinary ⋮ Rapid Review ⋮ Open Access Journal

Received October 20, 2020, accepted October 29, 2020, date of publication November 3, 2020, date of current version November 17, 2020.

Digital Object Identifier 10.1109/ACCESS.2020.3035602

Investigation on a New Discrete-Time Synchronous Motion Planning Scheme for Dual-Arm Robot Systems

TIE WANG[1], AND DONGSHENG GUO[2], (Member, IEEE)
[1]Logistics Management Department, Qiqihar Medical University, Qiqihar 161006, China
[2]College of Information Science and Engineering, Huaqiao University, Xiamen 361021, China

Corresponding author: Tie Wang (qqhr3977@163.com)

This work was supported in part by the Social Science Research Project of Qiqihar under Grant QSX2018-07YB, and in part by the Quanzhou City Science and Technology Program of China under Grant 2018C111R.

ABSTRACT Recently, the synchronous motion planning (SMP) has been viewed as a crucial issue in dual-arm robot systems. In this study, a new SMP scheme based on the Jacobian pseudoinverse formulation is presented and investigated for dual-arm robot systems. Such a scheme is established by discretizing the existing SMP scheme via a special difference formula. The presented discrete-time SMP (DTSMP) scheme is then theoretically analyzed to possess the biquadrate pattern in the end-effector planning error of each arm, thereby guaranteeing the synchronous planning precision of dual-arm robot systems. Simulation results under the system composed of two four-link planar robot arms are provided to further substantiate the effective and superior performance of the presented DTSMP scheme.

INDEX TERMS Synchronous motion planning, dual-arm robot systems, biquadrate pattern, planning precision, simulations.

I. INTRODUCTION

In recent years, the robot systems composed of two arms, i.e., dual-arm robot systems, have played a remarkable role in numerous fields [1]–[5]. In comparison with the single-arm robot system, the dual-arm robot system has more dexterity and flexibility, and thus can conduct more tasks requiring sophisticated motion and/or manipulation in complex environments. There are many benefits for dual-arm robot systems in industrial applications, such as synchronous motion for handling heavy loads, cooperative manipulation for completing multiple tasks, and cycle time improvement when keeping safe manipulation speed. Different types of dual-arm robot systems have been reported and investigated [6]–[10]. For example, a dual-arm robot system that consists of two 6-DOF (degrees-of-freedom) arms was developed in [7] for precision assembly. Another dual-arm robot system that is composed of two 7-DOF arms was designed in [8] for cell manufacturing process.

With regard to dual-arm robot systems, the synchronous motion planning (SMP), which can also be referred to as synchronous/cooperative kinematic control, is an interesting and active topic [1], [5], [9]–[13]. This topic is related to many practical application in industry, such as coordinate welding, cooperative assembling, and dextrous grasping. In general, the SMP of dual-arm robot systems can be described as that, given the desired path for the end-effector of each arm (to cooperatively perform, e.g., welding, assembling, and grasping), the related joint trajectory of each arm needs to be calculated accurately and determined simultaneously. Because of its significance, the SMP of dual-arm robot systems has recently been studied by many scientific researchers and engineering practitioners [1], [5], [9]–[25].

There are two general approaches for the SMP of dual-arm robot systems. The first one is based on the (relative) Jacobian pseudoinverse formulation [10], [15]–[21], where the SMP schemes are depicted as the summation of a minimum-norm particular solution and a homogeneous solution. The typical characteristic of this approach has made the related study popular in the past decades. For example, Lewis [16] introduced a relative Jacobian scheme for dual-arm robot systems, and a more compact expression of such scheme was presented by Jamisola Jr. and Roberts [17]. Hu *et al* [18] investigated another relative Jacobian scheme for dual-arm

The associate editor coordinating the review of this manuscript and approving it for publication was Jianyong Yao.

This work is licensed under a Creative Commons Attribution 4.0 License. For more information, see https://creativecommons.org/licenses/by/4.0/

robot systems under task conflicts and joint constraints. Freddi *et al* [10], [19], [20] developed many effective schemes with the Jacobian pseudoinverse formulation for dual-arm robot systems. The second approach for the SMP of dual-arm robot systems is based on the quadratic programming formulation [22]–[25]. In the study of this approach, the common way is to design an optimization performance index, formulate the end-effector planning requirement and physical limits as constraints, and thus establish the corresponding SMP schemes for dual-arm robot systems. These schemes can further be reformulated and unified into a quadratic program (QP) problem that can be solved by neural networks. By effectively calculating the QP problem, the SMP of dual-arm robot systems can eventually be achieved [22]–[25]. Notably, although remarkable success has been realized in the SMP of dual-arm robot systems, the existing literature mainly focuses on the SMP scheme design but the further improvement of the synchronous planning precision is generally neglected.

With regard to the SMP of dual-arm robot systems, an important issue that requires consideration is to guarantee and further improve the synchronous planning precision [7], [14]. For example, during the assembly process, we need to ensure the precision of cooperative manipulation by the dual-arm robot system [7]. By using the SMP scheme that has a potential of realizing high precision, the dual-arm robot system can cooperatively and accurately perform the particular task (e.g., assembling, welding, and grasping). Generally speaking, if the end-effector planning error of each arm can be kept within the region of a (sufficient) small value, then the (high) synchronous planing precision of the whole robot system can be guaranteed. Focus on improving the end-effector planning precision of one robot arm, Li *et al* [26] developed a novel recurrent neural network, and Guo *et al* [27] used a typical difference formula. Differing from such two methods, the methods based on auto disturbance rejection controller (ADRC) to improve the robot planning precision were investigated by Liu *et al* [28] and Humaidi *et al* [29]. In addition to the ADRC, the planning precision can also be effectively improved by designing and using other controllers, such as the extended-state-observer-based adaptive controller and the barrier function-based asymptotic tracking controller [30]–[34].

In this study, following the existing successful work [10], [14], [15], [27], [35], we show a further investigation on the SMP of dual-arm robot systems. That is, a new discrete-time SMP (DTSMP) scheme based on the pseudoinverse formulation is presented and investigated for dual-arm robot systems, where the end-effector planning precision of each arm can be guaranteed. The main contributions of this study are summarized and listed as follows.

i) A new DTSMP scheme for dual-arm robot systems is established by using a special difference formula [36]–[38] to discretize a previous SMP scheme. To the best of our knowledge, the presented DTSMP scheme has not been reported in existing literature.
ii) Theoretical analysis is provided to indicate the characteristic of the presented DTSMP scheme. Computer simulations are performed to verify the effectiveness of the presented DTSMP scheme.
iii) Results reveal that the presented DTSMP scheme possesses the biquadrate pattern in the end-effector planning error of each arm. Specifically, the planning error changes in the mode of $O(\sigma^4)$, where σ denotes the sampling gap.
iv) This study is the first attempt to provide an effective SMP scheme with biquadrate pattern in synchronous planning precision for dual-arm robot systems. This study is crucial, because it shows a new insight into the design of different SMP schemes for dual-arm robot systems with guaranteed precision.

The rest of this study is organized as follows: Section II presents some preliminaries about the SMP of dual-arm robot systems. Section III describes the new DTSMP scheme in this study for dual-arm robot systems, and provides the corresponding theoretical analysis. Section IV shows the simulation results under the robot system composed of two four-link planar arms, which are obtained with the presented DTSMP scheme. Section V concludes this study and presents the final remarks.

II. SYNCHRONOUS MOTION PLANNING

In this section, the description for the SMP of dual-arm robot systems is presented, and the SMP scheme with the pseudoinverse-based formulation is provided to lay a basis for further discussion.

A. PRELIMINARY

The SMP is a crucial issue in the study of dual-arm robot systems. Mathematically, the SMP of dual-arm robot systems can be realized by simultaneously and effectively solving the following nonlinear kinematic equation:

$$\begin{cases} f_{\mathrm{L}}(\theta_{\mathrm{L}}) = \phi_{\mathrm{L}} & \text{for the left arm,} \\ f_{\mathrm{R}}(\theta_{\mathrm{R}}) = \phi_{\mathrm{R}} & \text{for the right arm,} \end{cases} \tag{1}$$

where $\theta_{\{\mathrm{L,R}\}} \in R^n$ denote the joint-angle vectors of the left and right arms, $\phi_{\{\mathrm{L,R}\}} \in R^m$ denote the given end-effector desired paths, and $f_{\{\mathrm{L,R}\}}(\cdot) : R^n \to R^m$ denote the nonlinear mappings. In other words, given ϕ_{L} and ϕ_{R}, we need to solve for θ_{L} and θ_{R} via (1) simultaneously and accurately, such that the end-effectors of dual-arm robot systems can synchronously track the desired paths and cooperatively perform the specific tasks (e.g., welding, assembling, and grasping). Notably, in this study, we focus on the situation of $m < n$ for each arm in (1), which means that each arm considered in the robot system is a redundant one. In this situation, the possible joint-angle solution of each arm is infinite for a given end-effector desired path.

Because (1) is a nonlinear and underdetermined equation, it is generally difficult to obtain the solution of θ_{L} and θ_{R} by directly solving (1). Differentiating (1) with respect to time t

results in the linear relationship as follows:

$$\begin{cases} J_{\mathrm{L}}(\theta_{\mathrm{L}})\dot{\theta}_{\mathrm{L}} = \dot{\phi}_{\mathrm{L}} & \text{for the left arm,} \\ J_{\mathrm{R}}(\theta_{\mathrm{R}})\dot{\theta}_{\mathrm{R}} = \dot{\phi}_{\mathrm{R}} & \text{for the right arm,} \end{cases} \tag{2}$$

where $J_{\{\mathrm{L,R}\}} \in R^{m\times n}$ and $\dot{\theta}_{\{\mathrm{L,R}\}} \in R^{n}$ denote the Jacobian matrices and the joint-velocity vectors of the left and right arms, and $\dot{\phi}_{\{\mathrm{L,R}\}} \in R^{m}$ denote the time derivatives of $\phi_{\{\mathrm{L,R}\}}$. Notably, (2) is also underdetermined because of $n > m$, which means that the possible $\dot{\theta}_{\mathrm{L}}$ and $\dot{\theta}_{\mathrm{R}}$ solutions are infinite for the given ϕ_{L} and ϕ_{R}.

B. PSEUDOINVERSE-BASED SMP SCHEME

The approach based on the Jacobian pseudoinverse formulation has been developed and used to determine the $\dot{\theta}_{\mathrm{L}}$ and $\dot{\theta}_{\mathrm{R}}$ solutions for realizing the SMP of dual-arm robot systems [10], [15]–[21]. Specifically, with regard to (2), by introducing the feedback, the Jacobian pseudoinverse approach for dual-arm robot systems is formulated as follows:

$$\begin{cases} \dot{\theta}_{\mathrm{L}} = J_{\mathrm{L}}^{\dagger}(\theta_{\mathrm{L}})\big(\dot{\phi}_{\mathrm{L}} - k(f_{\mathrm{L}}(\theta_{\mathrm{L}}) - \phi_{\mathrm{L}})\big) + (I - J_{\mathrm{L}}^{\dagger}(\theta_{\mathrm{L}})J_{\mathrm{L}}(\theta_{\mathrm{L}}))c_{\mathrm{L}}, \\ \dot{\theta}_{\mathrm{R}} = J_{\mathrm{L}}^{\dagger}(\theta_{\mathrm{R}})\big(\dot{\phi}_{\mathrm{R}} - k(f_{\mathrm{R}}(\theta_{\mathrm{R}}) - \phi_{\mathrm{R}})\big) + (I - J_{\mathrm{R}}^{\dagger}(\theta_{\mathrm{R}})J_{\mathrm{R}}(\theta_{\mathrm{R}}))c_{\mathrm{R}}, \end{cases} \tag{3}$$

where $J_{\{\mathrm{L,R}\}}^{\dagger} \in R^{n\times m}$ denote the pseudoinverse matrices of $J_{\{\mathrm{L,R}\}}$, $k > 0 \in R$ denotes the feedback gain, $I \in R^{n\times n}$ denotes the identity matrix, and $c_{\{\mathrm{L,R}\}} \in R^{n}$ denote the vectors that are selected on the basis of some criteria [15]. Different selections of c_{L} and c_{R} in (3) lead to different schemes with specific characteristics (e.g., repetitive motion, singularity handling, or joint limit avoidance) for the SMP of dual-arm robot systems [10], [15].

In particular, by selecting $c_{\mathrm{L}} = c_{\mathrm{R}} = 0$, (3) is reduced to the following pseudoinverse-based SMP scheme for determining the $\dot{\theta}_{\mathrm{L}}$ and $\dot{\theta}_{\mathrm{R}}$ solutions of (2) simultaneously [35]:

$$\begin{cases} \dot{\theta}_{\mathrm{L}} = J_{\mathrm{L}}^{\dagger}(\theta_{\mathrm{L}})\big(\dot{\phi}_{\mathrm{L}} - k(f_{\mathrm{L}}(\theta_{\mathrm{L}}) - \phi_{\mathrm{L}})\big), \\ \dot{\theta}_{\mathrm{R}} = J_{\mathrm{R}}^{\dagger}(\theta_{\mathrm{R}})\big(\dot{\phi}_{\mathrm{R}} - k(f_{\mathrm{R}}(\theta_{\mathrm{R}}) - \phi_{\mathrm{R}})\big). \end{cases} \tag{4}$$

For presentation convenience, the pseudoinverse-based SMP scheme (4) is transformed into the unified form as follows:

$$\dot{\vartheta} = P(\vartheta)\big(\dot{\varphi} - k(\mathcal{F}(\vartheta) - \varphi)\big), \tag{5}$$

where the augmented vectors and matrix are given by

$$\dot{\vartheta} = \begin{bmatrix} \dot{\theta}_{\mathrm{L}} \\ \dot{\theta}_{\mathrm{R}} \end{bmatrix} \in R^{2n}, \quad \vartheta = \begin{bmatrix} \theta_{\mathrm{L}} \\ \theta_{\mathrm{R}} \end{bmatrix} \in R^{2n}, \quad \dot{\varphi} = \begin{bmatrix} \dot{\phi}_{\mathrm{L}} \\ \dot{\phi}_{\mathrm{R}} \end{bmatrix} \in R^{2m},$$
$$\varphi = \begin{bmatrix} \phi_{\mathrm{L}} \\ \phi_{\mathrm{R}} \end{bmatrix} \in R^{2m}, \quad \mathcal{F}(\vartheta) = \begin{bmatrix} f_{\mathrm{L}}(\theta_{\mathrm{L}}) \\ f_{\mathrm{R}}(\theta_{\mathrm{R}}) \end{bmatrix} \in R^{2m}, \text{ and}$$
$$P(\vartheta) = \begin{bmatrix} J_{\mathrm{L}}^{\dagger}(\theta_{\mathrm{L}}) & 0 \\ 0 & J_{\mathrm{R}}^{\dagger}(\theta_{\mathrm{R}}) \end{bmatrix} \in R^{2n\times 2m}.$$

With regard to the pseudoinverse-based SMP scheme (5), an alternative for this scheme is to use the MATLAB routine "ODE" [39], thereby obtaining the corresponding solutions of θ_{L} and θ_{R} in (1). Furthermore, since (5) is depicted in a continuous-time form, the Euler difference formula [40], which is a widely-used formula, can be utilized to discretize (5). The resultant scheme with discrete-time form is developed to determine the θ_{L} and θ_{R} solutions at each time instant for realizing the SMP of dual-arm robot systems. However, this scheme may be ineffective in guaranteeing the (high) planning precision for dual-arm robot systems, which will be presented in Section IV.

III. NEW DTSMP SCHEME

In this section, a special difference formula in [36]–[38] is presented and used to discretize the pseudoinverse-based scheme (5). The new DTSMP scheme is thus established for dual-arm robot systems with guaranteed precision. Theoretical analysis of such a new scheme is provided as well.

A. SCHEME FORMULATION

In [36]–[38], the difference formula is established for first-order derivative approximation, which is written as follows:

$$\dot{\chi}(t_k) = \big(24\chi(t_{k+1}) - 5\chi(t_k) - 12\chi(t_{k-1}) - 6\chi(t_{k-2}) - 4\chi(t_{k-3}) + 3\chi(t_{k-4})\big)/(48\sigma) + O(\sigma^3), \tag{6}$$

where the sampling gap $\sigma = t_{k+1} - t_k = t_k - t_{k-1} = t_{k-1} - t_{k-2} = t_{k-2} - t_{k-3} = t_{k-3} - t_{k-4}$ with $k = 4, 5, 6, \cdots$. It follows from the difference formula (6) that the approximation of the combined joint velocity $\dot{\vartheta}_k = \dot{\vartheta}(t_k = k\sigma)$ in (5) at time instant t_k is given by

$$\dot{\vartheta}(t_k) = \big(24\vartheta(t_{k+1}) - 5\vartheta(t_k) - 12\vartheta(t_{k-1}) - 6\vartheta(t_{k-2}) - 4\vartheta(t_{k-3}) + 3\vartheta(t_{k-4})\big)/(48\sigma) + O(\sigma^3), \tag{7}$$

with $\vartheta_k = \vartheta(t_k = k\sigma)$ and the initial time instant $t_0 = 0$ s.

Using (7) to discretize the pseudoinverse-based scheme (5) results in the following formulation:

$$\vartheta_{k+1} = \frac{5}{24}\vartheta_k + \frac{1}{2}\vartheta_{k-1} + \frac{1}{4}\vartheta_{k-2} + \frac{1}{6}\vartheta_{k-3} - \frac{1}{8}\vartheta_{k-4} + P(\vartheta_k)\big(2\sigma\dot{\varphi}_k - h(\mathcal{F}(\vartheta_k) - \varphi_k)\big) + O(\sigma^4), \tag{8}$$

where $\dot{\varphi}_k = \dot{\varphi}(t_k = k\sigma)$, $\varphi_k = \varphi(t_k = k\sigma)$, and $h = 2\sigma k > 0 \in R$ denotes the step size. The elimination of the error term $O(\sigma^4)$ in (8) further yields

$$\vartheta_{k+1} = \frac{5}{24}\vartheta_k + \frac{1}{2}\vartheta_{k-1} + \frac{1}{4}\vartheta_{k-2} + \frac{1}{6}\vartheta_{k-3} - \frac{1}{8}\vartheta_{k-4} + P(\vartheta_k)\big(2\sigma\dot{\varphi}_k - h(\mathcal{F}(\vartheta_k) - \varphi_k)\big), \tag{9}$$

which is called the new DTSMP scheme for dual-arm robot systems in this study. By following the above derivation, the presented DTSMP scheme (9) has a truncation error of $O(\sigma^4)$.

With regard to (9), we need five states (i.e., ϑ_0, ϑ_1, ϑ_2, ϑ_3, and ϑ_4) to start the recursion. In this situation, given the initial joint states $\theta_{\mathrm{L}0}$ and $\theta_{\mathrm{R}0}$ of both arms, we have $\vartheta_0 = [\theta_{\mathrm{L}0}; \theta_{\mathrm{R}0}]$, and further have the other states by the following

calculation:

$$\begin{cases} \vartheta_1 = \vartheta_0 + P(\vartheta_0)\big(\sigma\dot{\varphi}_0 - h(\mathcal{F}(\vartheta_0) - \varphi_0)\big), \\ \vartheta_2 = \vartheta_1 + P(\vartheta_1)\big(\sigma\dot{\varphi}_1 - h(\mathcal{F}(\vartheta_1) - \varphi_1)\big), \\ \vartheta_3 = \vartheta_2 + P(\vartheta_2)\big(\sigma\dot{\varphi}_2 - h(\mathcal{F}(\vartheta_2) - \varphi_2)\big), \\ \vartheta_4 = \vartheta_3 + P(\vartheta_3)\big(\sigma\dot{\varphi}_3 - h(\mathcal{F}(\vartheta_3) - \varphi_3)\big). \end{cases}$$

In summary, with five pre-calculated states, the presented DTSMP scheme (9) would generate the corresponding sequence $\{\vartheta_k\}$ (with $k = 0, 1, \cdots, T/\sigma$, and T denoting the task duration), which constitutes the θ_{L} and θ_{R} solutions of (1), to realize the SMP of dual-arm robot systems.

B. THEORETICAL ANALYSIS

In this subsection, the presented DTSMP scheme (9) is theoretically analyzed to possess the biquadrate pattern in the end-effector planning error of each arm, thereby guaranteeing the synchronous planning precision of dual-arm robot systems.

Lemma 1: The presented DTSMP scheme (9) has the property of zero stability and consistency, thus having the property of convergence.

Proof: The zero-stability property of (9) is analyzed by the following characteristic polynomial [41]:

$$\psi(\rho) = \rho^5 - \frac{5}{24}\rho^4 - \frac{1}{2}\rho^3 - \frac{1}{4}\rho^2 - \frac{1}{6}\rho + \frac{1}{8}.$$

As presented in [36]–[38], the roots of $\psi(\rho) = 0$ are on or in the unit circle, which indicates that (9) is zero stable. As analyzed in Section III-A, (9) has a truncation error of $O(\sigma^4)$, thereby indicating its consistency property. On the basis of [41], the properties of being simultaneously zero stable and consistent will eventually lead to the convergence property of the presented DTSMP scheme (9). The proof is thus completed. ■

In mathematics, Lemma 1 shows that the solution of ϑ_k generated by (9) would converge to a theoretical solution denoted by $\vartheta_k^* = \vartheta^*(t_k = k\delta)$ (which satisfies $\mathcal{F}(\vartheta_k^*) - \varphi_k = 0$). Furthermore, the following relationship between such two solutions is obtained with a sufficiently large k value:

$$\vartheta_k = \vartheta_k^* + O(\sigma^4). \tag{10}$$

In this sense, Lemma 1 confirms the effective performance of the presented DTSMP scheme (9) in dual-arm robot systems.

Lemma 2: Considering dual-arm robot systems with no singularity and collision happened, the end-effector planning error of each arm via the presented DTSMP scheme (9) changes in the mode of $O(\sigma^4)$.

Proof: Let us recall (10). When the value of k is sufficiently large, the following result is obtained:

$$\begin{aligned} \mathcal{F}(\vartheta_k) - \varphi_k &= \mathcal{F}(\vartheta_k^* + O(\sigma^4)) - \varphi_k \\ &= \mathcal{F}(\vartheta_k^*) - \varphi_k + O(\sigma^4) = O(\sigma^4). \end{aligned} \tag{11}$$

Let us recall the definitions of $\mathcal{F}(\vartheta)$ and φ in Section II-B. Then, the reformulation of (11) is given by

$$\begin{cases} \varepsilon_{\mathrm{L}k} = f_{\mathrm{L}}(\theta_{\mathrm{L}k}) - \phi_{\mathrm{L}k} = O(\sigma^4), \\ \varepsilon_{\mathrm{R}k} = f_{\mathrm{R}}(\theta_{\mathrm{R}k}) - \phi_{\mathrm{R}k} = O(\sigma^4), \end{cases} \tag{12}$$

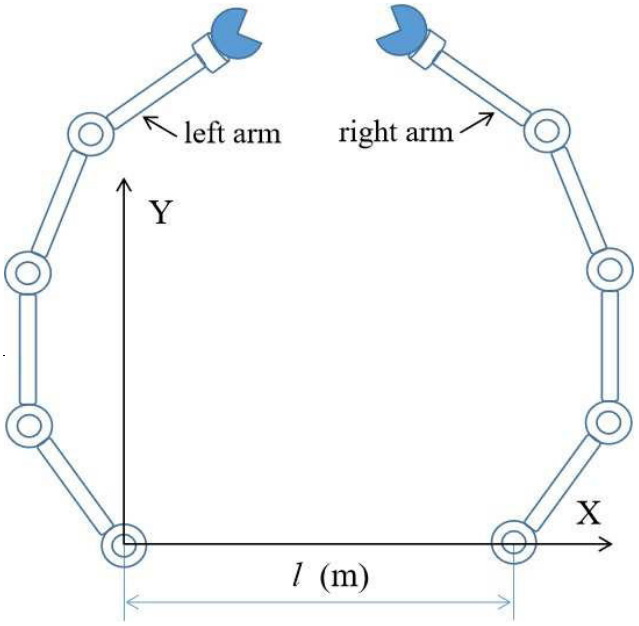

FIGURE 1. A dual-arm robot system composed of two four-link planar arms.

where $\varepsilon_{\mathrm{L}k}$ and $\varepsilon_{\mathrm{R}k}$ denote the end-effector planning errors of the left and right arms computed by (9) at time instant t_k. It follows from (12) that the end-effector planning error of each arm via (9) changes in the mode of $O(\sigma^4)$. This statement also indicates that the presented DTSMP scheme (9) possess the biquadrate pattern in the end-effector planning error of each arm. The proof is thus completed. ■

Remarks: The above theoretical analysis confirms that the end-effector planning error of each arm (i.e., $\varepsilon_{\mathrm{L}k}$ and $\varepsilon_{\mathrm{R}k}$) computed by the presented DTSMP scheme (9) occurs without divergence. Furthermore, because of the $O(\sigma^4)$ mode in (12), the magnitude of $\varepsilon_{\mathrm{L}k}$ and $\varepsilon_{\mathrm{R}k}$ can be maintained within the region of a (very) small value by using an appropriate value of σ in (9). This point will be presented and discussed in Section IV. In summary, Lemmas 1 and 2 indicate that the presented DTSMP scheme (9) can theoretically guarantee the precision of end-effector planning for each arm, and thus achieve the (high) synchronous planning precision of dual-arm robot systems.

IV. SIMULATION COMPARISON AND VALIDATION

In this section, comparative simulation results under a dual-arm robot system are provided to substantiate the effectiveness of the presented DTSMP scheme (9). For better understanding, the robot system that is composed of two four-link planar arms is shown in Fig. 1, where both arms are located at the same plane.

A. SYNCHRONOUS MOTION

In this subsection, the presented DTSMP scheme (9) is investigated with two illustrative examples.

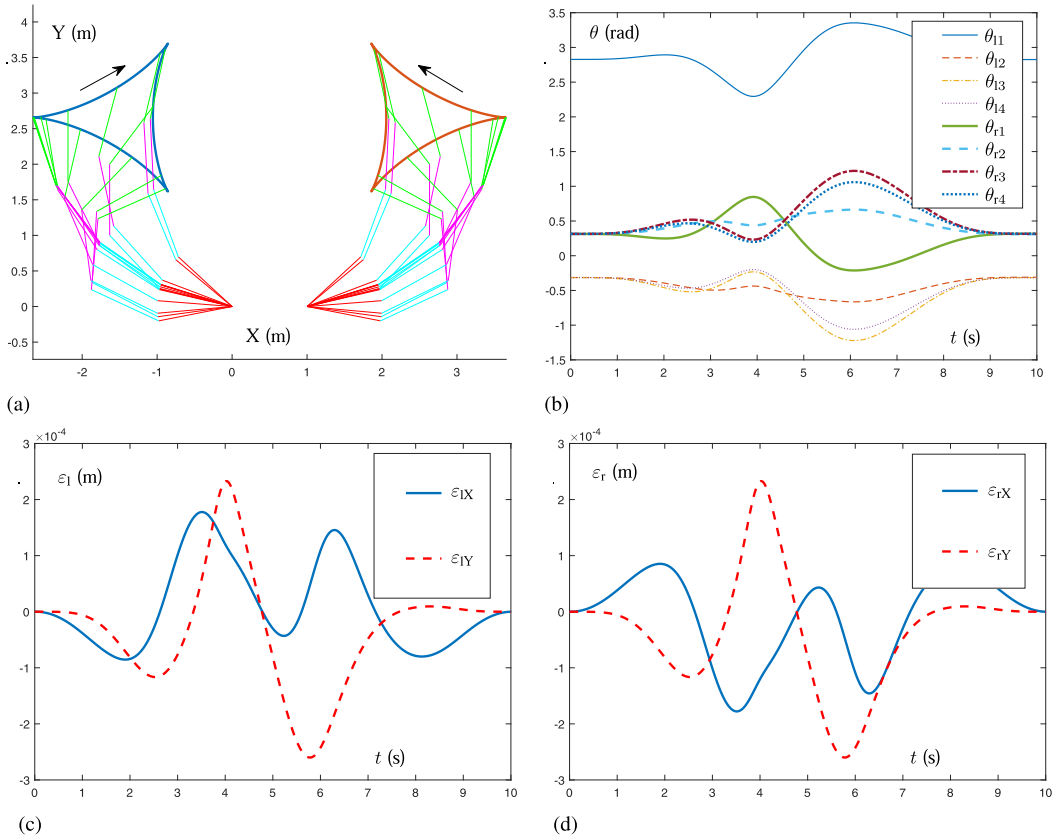

FIGURE 2. Simulation results of the dual-arm robot system using the SMP scheme (13) with $\sigma = 0.01$ and $h = 0.4$ for both end-effectors simultaneously tracking the same tricuspid path, where time $t \in \{0, \sigma, 2\sigma, \cdots, 10\}$ s. (a) Synchronous motion trajectories. (b) Joint angle trajectories. (c) End-effector planning errors of left arm. (d) End-effector planning errors of right arm.

Example A.1: In this example, we simulate the presented DTSMP scheme (9) under the dual-arm robot system, where the end-effectors of both arms are expect to simultaneously track the same tricuspid path. In the simulations, the joint initial states of the left and right arms are set respectively as $\theta_{\mathrm{L}0} = [9\pi/10; -\pi/10; -\pi/10; -\pi/10]$ rad and $\theta_{\mathrm{R}0} = [\pi/10; \pi/10; \pi/10; \pi/10]$ rad, and the motion duration is set as $T = 10$ s. For comparison, the following SMP scheme, which can be derived from the discretization of (5) using the Euler difference formula [40], is also simulated:

$$\vartheta_{k+1} = \vartheta_k + P(\vartheta_k)\big(\sigma\dot{\varphi}_k - h(\mathcal{F}(\vartheta_k) - \varphi_k)\big). \qquad (13)$$

Fig. 2 shows the simulation results of the dual-arm robot system using the SMP scheme (13) with $\sigma = 0.01$ and $h = 0.4$, where time $t \in \{0, \sigma, 2\sigma, \cdots, 10\}$ s, and the end-effector planning errors of the left and right arms at each time instant are obtained with $\varepsilon_{\mathrm{L}k} = f_{\mathrm{L}}(\theta_{\mathrm{L}k}) - \phi_{\mathrm{L}k} \in R^2$ and $\varepsilon_{\mathrm{R}k} = f_{\mathrm{R}}(\theta_{\mathrm{R}k}) - \phi_{\mathrm{R}k} \in R^2$. As shown in Fig. 2, the end-effector of each arm successfully tracks the desired path with the maximal planning error being less than 3×10^{-4} m. This result indicates that (13) effectively enables the SMP of the dual-arm robot system.

By contrast, Fig. 3 presents the simulation results of the dual-arm robot system using the presented DTSMP scheme (9) with $\sigma = 0.01$ and $h = 0.4$. As presented in Fig. 3, the end-effector of each arm also successfully tracks the desired path with the maximal planning error being less than 4×10^{-7} m. Figs. 3(c) and (d) further present that the end-effector planning errors of both arms do not exhibit divergence. These results reflect the effective performance of (9) in realizing the SMP of the dual-arm robot system. Moreover, comparing Figs. 2 and 3 reveals that the maximal end-effector planning error of each arm via (9) is approximately $1,000$ times smaller than that via (13), i.e., 10^{-7} versus 10^{-4}. Therefore, the presented DTSMP scheme (9) is advantageous over the SMP scheme (13) for the dual-arm robot system.

By decreasing the value of σ from 0.01 to 0.001, both the SMP schemes (9) and (13) are simulated, and the corresponding results are shown in Figs. 4 and 5. Evidently, these simulation results verify again the effectiveness of (9) and (13) in terms of a small end-effector planning error. In addition, a comparison of Figs. 2 and 4 reveals that the maximal planning error of each arm via (13) is reduced by 100 times with decrease in σ by 10 times (i.e., from 10^{-4} m to 10^{-6} m). Another comparison of Figs. 3 and 5 reveals that the maximal planning error of each arm via (9) is reduced by $10,000$ times with decrease in σ by 10 times (i.e., from 10^{-7} m to 10^{-11} m). These comparative results show that the

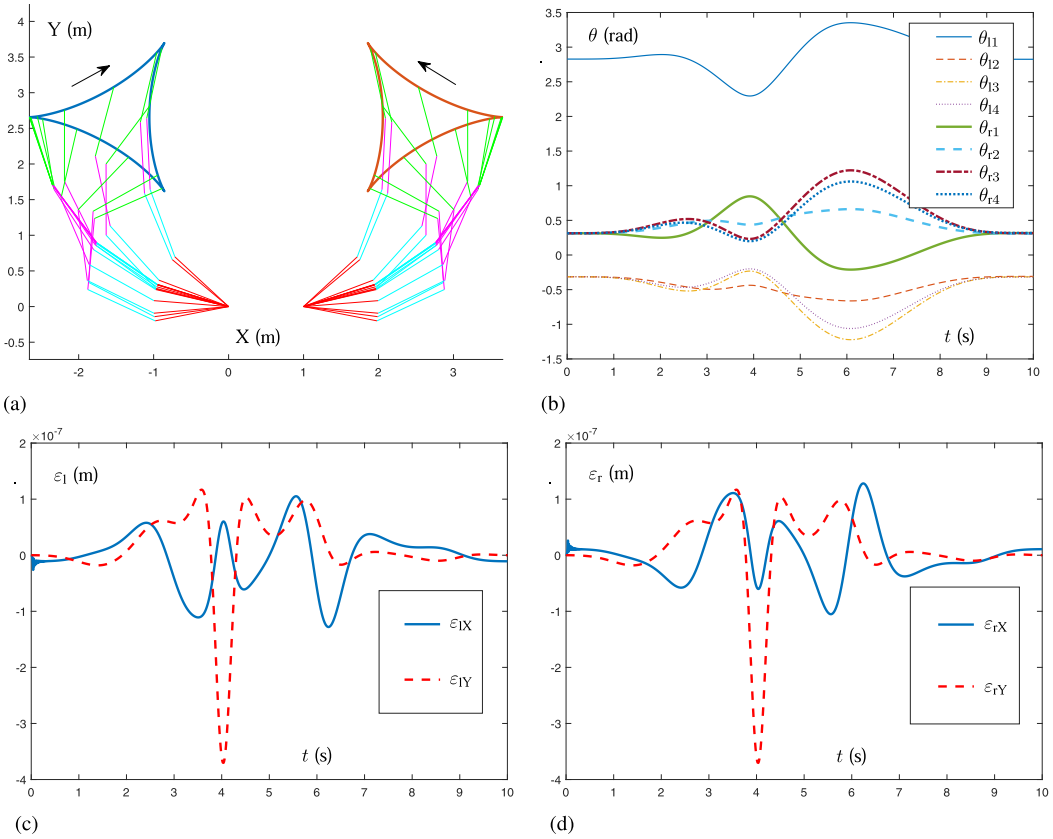

FIGURE 3. Simulation results of the dual-arm robot system using the presented DTSMP scheme (9) with $\sigma = 0.01$ and $h = 0.4$ for both end-effectors simultaneously tracking the same tricuspid path. (a) Synchronous motion trajectories. (b) Joint angle trajectories. (c) End-effector planning errors of left arm. (d) End-effector planning errors of right arm.

TABLE 1. Maximal end-effector planning errors of the dual-arm robot system using the presented DTSMP scheme (9) with different σ and h for one end-effector tracking the tricuspid path and the other tracking the astroid path.

#	h	$\sigma = 0.02$	$\sigma = 0.01$	$\sigma = 0.002$	$\sigma = 0.001$	Changing mode
Left arm	0.2	5.293×10^{-6}	3.947×10^{-7}	6.931×10^{-10}	4.348×10^{-11}	$O(\sigma^4)$
	0.3	3.979×10^{-6}	2.764×10^{-7}	4.634×10^{-10}	2.901×10^{-11}	
	0.4	3.157×10^{-6}	2.115×10^{-7}	3.479×10^{-10}	2.176×10^{-11}	
	0.5	2.603×10^{-6}	1.709×10^{-7}	2.784×10^{-10}	1.741×10^{-11}	
	0.6	2.209×10^{-6}	1.432×10^{-7}	2.321×10^{-10}	1.451×10^{-11}	
Right arm	0.2	1.381×10^{-5}	1.233×10^{-6}	2.602×10^{-9}	1.652×10^{-10}	$O(\sigma^4)$
	0.3	1.158×10^{-5}	9.351×10^{-7}	1.755×10^{-9}	1.105×10^{-10}	
	0.4	9.822×10^{-6}	7.450×10^{-7}	1.322×10^{-9}	8.295×10^{-11}	
	0.5	8.489×10^{-6}	6.165×10^{-7}	1.060×10^{-9}	6.639×10^{-11}	
	0.6	7.417×10^{-6}	5.237×10^{-7}	8.840×10^{-10}	5.534×10^{-11}	

presented DTSMP scheme (9) can generate a (much) smaller end-effector planning error than the SMP scheme (13) for the dual-arm robot system. A high planning precision of the dual-arm robot system using (9) is thus guaranteed and achieved.

In summary, the above simulation results (i.e., Figs. 2–5) verify the effective and superior performance of the presented DTSMP scheme (9) on the dual-arm robot system.

Example A.2: In this example, we simulate the presented DTSMP scheme (9) under the dual-arm robot system, where one end-effector is expect to track the tricuspid path and the other is expect to track the astroid path. In the simulations, the joint initial states of the left and right arms are set respectively as $\theta_{\mathrm{L}0} = [11\pi/12; -\pi/12; -\pi/12; -\pi/12]$ rad and $\theta_{\mathrm{R}0} = [\pi/12; \pi/12; \pi/12; \pi/12]$ rad, and the motion duration is set as $T = 10$ s.

Fig. 6 shows the simulation results of the dual-arm robot system using the presented DTSMP scheme (9) with $\sigma = 0.01$ and $h = 0.4$. As shown in Fig. 6, the end-effector of each arm effectively tracks the corresponding desired path. The maximal planning errors of the left and right arms are less

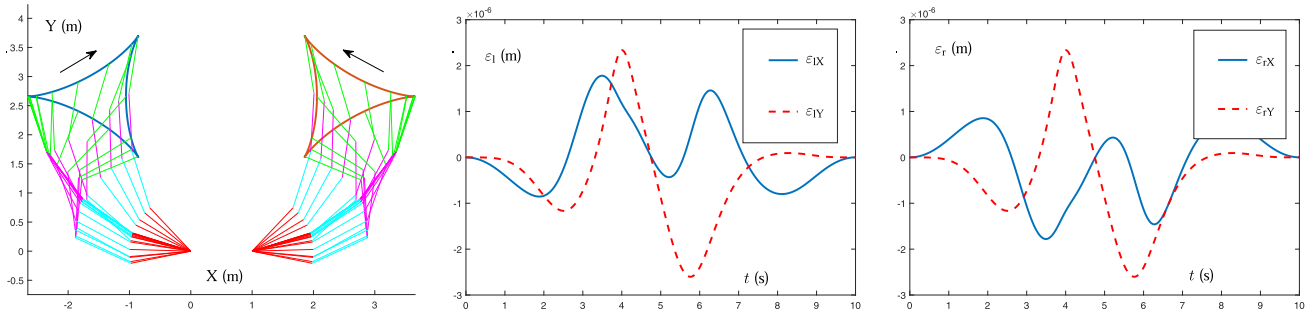

(a) (b) (c)

FIGURE 4. Simulation results of the dual-arm robot system using the SMP scheme (13) with $\sigma = 0.001$ and $h = 0.4$ for both end-effectors simultaneously tracking the tricuspid path. (a) Synchronous motion trajectories. (b) End-effector planning errors of left arm. (c) End-effector planning errors of right arm.

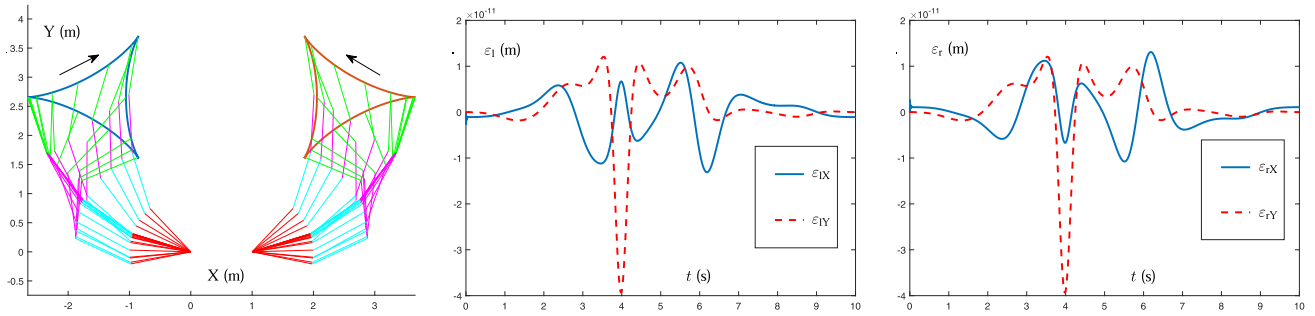

(a) (b) (c)

FIGURE 5. Simulation results of the dual-arm robot system using the presented DTSMP scheme (9) with $\sigma = 0.001$ and $h = 0.4$ for both end-effectors simultaneously tracking the tricuspid path. (a) Synchronous motion trajectories. (b) End-effector planning errors of left arm. (c) End-effector planning errors of right arm.

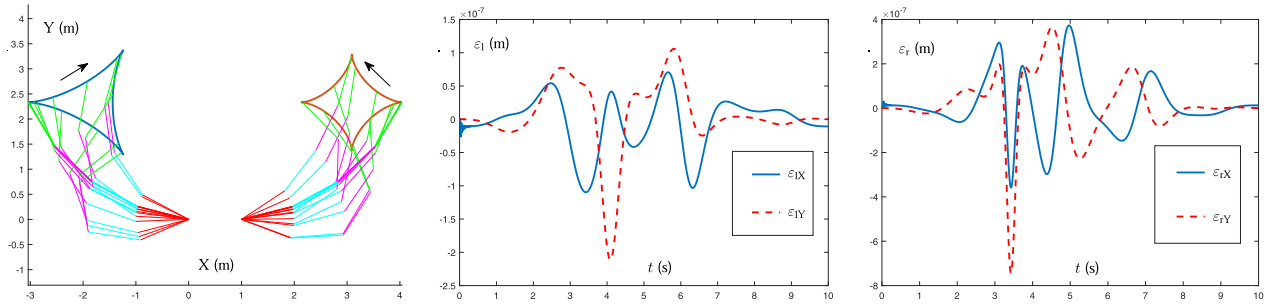

(a) (b) (c)

FIGURE 6. Simulation results of the dual-arm robot system using the presented DTSMP scheme (9) with $\sigma = 0.01$ and $h = 0.4$ for one end-effector tracking the tricuspid path and the other tracking the astroid path. (a) Synchronous motion trajectories. (b) End-effector planning errors of left arm. (c) End-effector planning errors of right arm.

than 2.5×10^{-7} m and 8×10^{-7} m, respectively. In addition, the end-effector planning errors of both arms do not encounter the divergence issue. These results confirm the effectiveness of the presented DTSMP scheme (9).

For further investigation, the presented DTSMP scheme (9) with different values of σ and h is simulated, and the related data are presented in Table 1. These data show that the SMP of the dual-arm robot system using (9) is successfully realized in the light of the small planning error of each arm. Moreover, the observed results from Table 1 are summarized as follows.

i) The sampling gap σ mainly affects the maximal end-effector planning error of each arm computed by the presented DTSMP scheme (9). With a fixed h, the maximal planning error is effectively reduced by decreasing σ.

ii) The end-effector planning precision of each arm via the presented DTSMP scheme (9) changes in the mode of $O(\sigma^4)$. Specifically, the decrease in σ by 10 times leads to the planning precision improvement by 10, 000 times. This observation coincides with the result stated in Lemma 2.

iii) A non-zero value of the step size h is to guarantee the end-effector planning error of each arm computed by the presented DTSMP scheme (9) with no divergence. Increasing h within an appropriate range can further improve the end-effector planning precision of each arm.

On the basis of these results, a small value of σ and a relatively large value of h in (9) can guarantee and achieve a high planning precision of dual-arm robot system, thereby

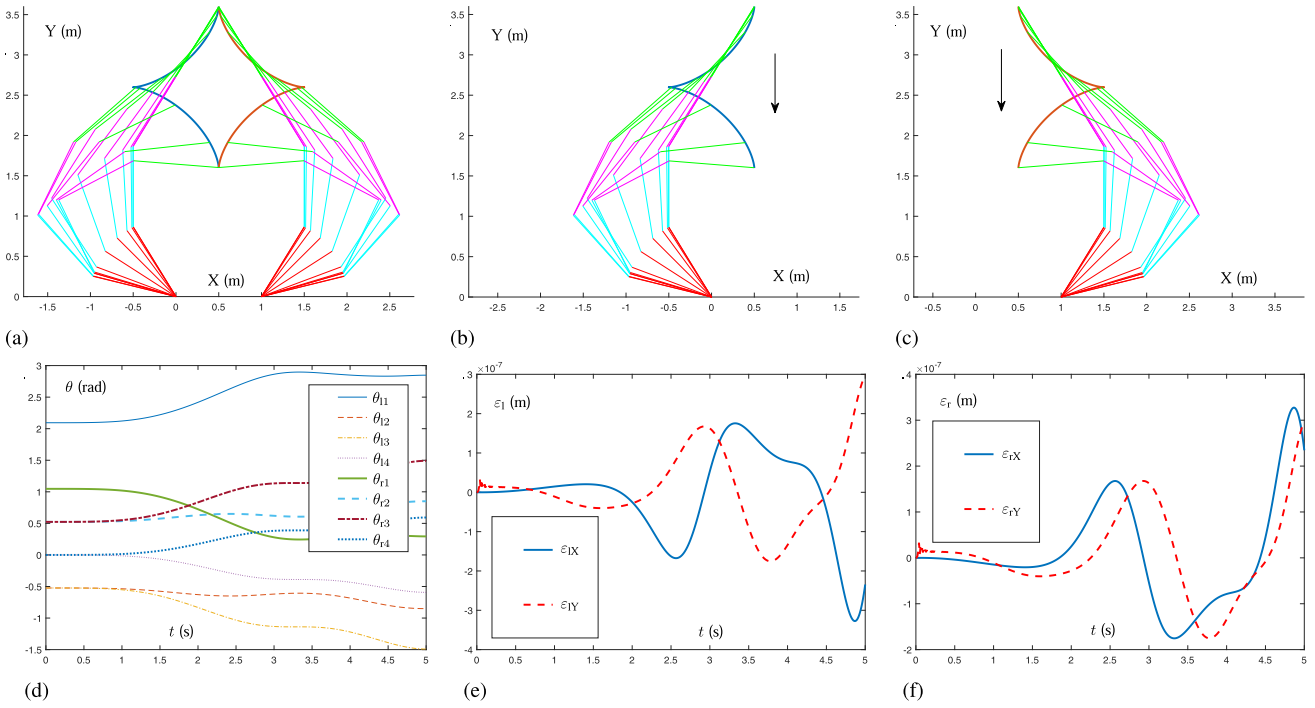

FIGURE 7. Simulation results of the dual-arm robot system using the presented DTSMP scheme (9) with $\sigma = 0.01$ and $h = 0.4$ for both end-effectors cooperatively tracking the astroid path. (a) Cooperative motion trajectories. (b) Motion trajectories of left arm. (c) Motion trajectories of right arm. (d) Joint angle trajectories. (e) End-effector planning errors of left arm. (f) End-effector planning errors of right arm.

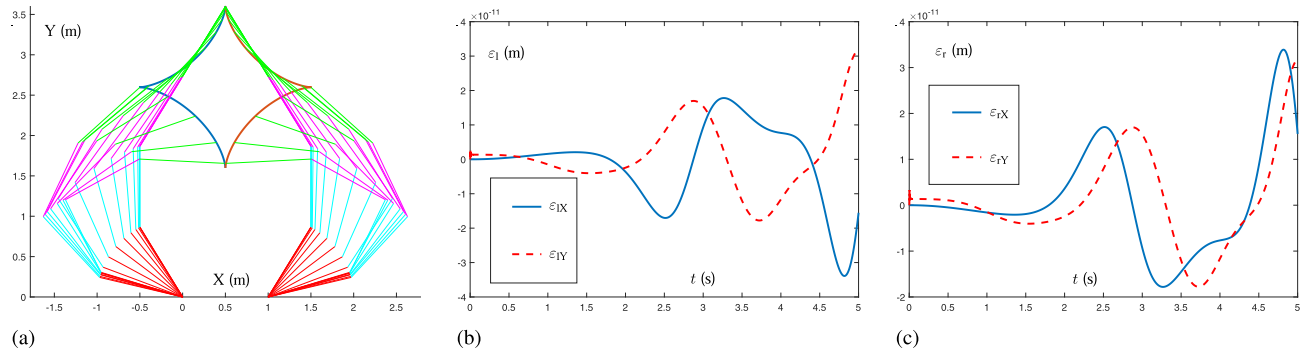

FIGURE 8. Simulation results of the dual-arm robot system using the presented DTSMP scheme (9) with $\sigma = 0.001$ and $h = 0.4$ for both end-effectors cooperatively tracking the astroid path. (a) Cooperative motion trajectories. (b) End-effector planning errors of left arm. (c) End-effector planning errors of right arm.

indicating the effective and superior performance of the presented DTSMP scheme (9).

B. COOPERATIVE MANIPULATION

In this subsection, the presented DTSMP scheme (9) is investigated under the dual-arm robot system, where the end-effectors of both arm are expect to cooperatively track the astroid path. In the simulations, the joint initial states of the left and right arms are set respectively as $\theta_{L0} = [2\pi/3; -\pi/6; -\pi/6; 0]$ rad and $\theta_{R0} = [\pi/3; \pi/6; \pi/6; 0]$ rad, and the motion duration is set as $T = 5$ s.

Fig. 7 presents the simulation results of the dual-arm robot system using the presented DTSMP scheme (9) with $\sigma = 0.01$ and $h = 0.4$. As presented in Fig. 7(a)-(c), the end-effector of each arms effectively track its corresponding path, and both arm finish tracking cooperatively the desired astroid path. As presented in Fig. 7(d)-(f), the maximal end-effector planning error of each arm computed by (9) is less than 4×10^{-7} m. This statement means that the astroid path tracking task is completed successfully via the dual-arm robot system with the cooperative manipulation. Evidently, the task execution time can be shorten greatly by the dual-arm robot system, as compared with the single-arm robot system (e.g., see the simulation result of the right arm in Fig. 6). These results show the advantage of the dual-arm robot system, and indicate the effectiveness of the presented DTSMP scheme (9).

With the decrease in σ (i.e., from 0.01 to 0.001), the presented DTSMP scheme (9) is simulated. The corresponding results are shown in Fig. 8, which verify again that (9) effectively enables the SMP of the dual-arm robot system. Moreover, a detailed inspection on Figs. 7 and 8 reveals that the end-effector planning precision of each arm via (9) changes in the mode of $O(\sigma^4)$. Specifically, with regard to each arm, its end-effector planning error is reduced by 10, 000 times; i.e., from 10^{-7} m to 10^{-11} m, when decreasing σ by 10 times. Therefore, the high planning precision of the dual-arm robot system using (9) is guaranteed and achieved.

In summary, these simulation results (i.e., Figs. 7 and 8) substantiate again the effective and superior performance of the presented DTSMP scheme (9) on the dual-arm robot system.

V. CONCLUSION

In this study, the SMP of dual-arm robot systems is investigated by presenting the new DTSMP scheme (9). Such a scheme is established from the discretization of the SMP scheme (5) using the special difference formula (7). It is then theoretically analyzed that the presented DTSMP scheme (9) possesses the biquadrate pattern in the end-effector planning error of each arm. Specifically, the planning error changes in the mode of $O(\sigma^4)$, which can guarantee the synchronous planning precision of dual-arm robot systems. On the basis of under the robot system composed of two four-link planar arms, comparative simulation results with different illustrative examples further indicate the effectiveness and superiority of the presented DTSMP scheme (9).

As for dual-arm robot systems, one future research direction can be the study of designing the SMP schemes by using the approach of neural networks [42]–[44]. Another future research direction can be the study of designing the SMP schemes by considering the handle of additive noise, environmental obstacle, and/or physical limits [45]–[47]. By following this study, the presented DTSMP scheme (9) is expected to be implemented on the real dual-arm robot system that consists of two practical EFORT robot manipulators.

ACKNOWLEDGMENT

The authors would like to thank the editors and anonymous reviewers for the time and effort spent in handling this study and constructive comments provided to improve the presentation and quality.

REFERENCES

[1] C. Smith, Y. Karayiannidis, L. Nalpantidis, X. Gratal, P. Qi, D. V. Di-marogonas, and D. Kragic, "Dual arm manipulation—A survey," *Robot. Auton. Syst.*, vol. 60, no. 10, pp. 1340–1353, 2012.

[2] E. Tuci, M. H. M. Alkilabi, and O. Akanyeti, "Cooperative object transport in multi-robot systems: A review of the State-of-the-Art," *Frontiers Robot. AI*, vol. 5, pp. 1–15, May 2018.

[3] D. Kragic, J. Gustafson, H. Karaoguz, P. Jensfelt, and R. Krug, "Interactive, collaborative robots: Challenges and opportunities," in *Proc. 27th Int. Joint Conf. Artif. Intell.*, Jul. 2018, pp. 18–25.

[4] D. Nicolis, M. Palumbo, A. M. Zanchettin, and P. Rocco, "Occlusion-free visual servoing for the shared autonomy teleoperation of dual-arm robots," *IEEE Robot. Autom. Lett.*, vol. 3, no. 2, pp. 796–803, Apr. 2018.

[5] W. Wan, K. Harada, and F. Kanehiro, "Preparatory manipulation planning using automatically determined single and dual arm," *IEEE Trans. Ind. Informat.*, vol. 16, no. 1, pp. 442–453, Jan. 2020.

[6] D. H. Song, W. K. Lee, and S. Jung, "Kinematics analysis and implementation of a motion-following task for a humanoid slave robot controlled by an exoskeleton master robot," *Int. J. Control, Automat., Syst.*, vol. 5, no. 6, pp. 681–690, 2007.

[7] C. Park and K. Park, "Design and kinematics analysis of dual arm robot manipulator for precision assembly," in *Proc. 6th IEEE Int. Conf. Ind. Informat.*, Jul. 2008, pp. 430–435.

[8] H. M. Do, C. Park, T. Y. Choi, and J. H. Kyung, "Design and control of dual-arm robot for cell manufacturing process," in *Proc. IEEE Int. Conf. Mechatronics Autom.*, Aug. 2013, pp. 1419–1423.

[9] S. Tarbouriech, B. Navarro, P. Fraisse, A. Crosnier, A. Cherubini, and D. Salle, "Dual-arm relative tasks performance using sparse kinematic control," in *Proc. IEEE/RSJ Int. Conf. Intell. Robots Syst. (IROS)*, Oct. 2018, pp. 6003–6008.

[10] D. Ortenzi, R. Muthusamy, A. Freddi, A. Monteriù, and V. Kyrki, "Dual-arm cooperative manipulation under joint limit constraints," *Robot. Auto. Syst.*, vol. 99, pp. 110–120, Jan. 2018.

[11] J. K. Behrens, K. Stepanova, R. Lange, and R. Skoviera, "Specifying dual-arm robot planning problems through natural language and demonstration," *IEEE Robot. Autom. Lett.*, vol. 4, no. 3, pp. 2622–2629, Jul. 2019.

[12] W. Xu, Y. Liu, and Y. Xu, "The coordinated motion planning of a dual-arm space robot for target capturing," *Robotica*, vol. 30, no. 5, pp. 755–771, Sep. 2012.

[13] Y. Gan, X. Dai, and J. Li, "Cooperative path planning and constraints analysis for master-slave industrial robots," *Int. J. Adv. Robotic Syst.*, vol. 8, pp. 88–100, 2012.

[14] C. Yang, Y. Jiang, Z. Li, W. He, and C.-Y. Su, "Neural control of bimanual robots with guaranteed global stability and motion precision," *IEEE Trans. Ind. Informat.*, vol. 13, no. 3, pp. 1162–1171, Jun. 2017.

[15] B. Siciliano, L. Sciavicco, L. Villani, and G. Oriolo, *Robotics: Modeling, Planning and Control*. London, U.K.: Springer-Verlag, 2009.

[16] C. L. Lewis, "Trajectory generation for two robots cooperating to perform a task," in *Proc. IEEE Int. Conf. Robot. Autom.*, Apr. 1996, pp. 1626–1631.

[17] R. S. Jamisola and R. G. Roberts, "A more compact expression of relative jacobian based on individual manipulator jacobians," *Robot. Auto. Syst.*, vol. 63, pp. 158–164, Jan. 2015.

[18] Y. Hu, B. Huang, and G.-Z. Yang, "Task-priority redundancy resolution for co-operative control under task conflicts and joint constraints," in *Proc. IEEE/RSJ Int. Conf. Intell. Robots Syst. (IROS)*, Sep. 2015, pp. 2398–2405.

[19] A. Freddi, S. Longhi, A. Monteriù, and D. Ortenzi, "Redundancy analysis of cooperative dual-arm manipulators," *Int. J. Adv. Robotic Syst.*, vol. 13, no. 5, pp. 1–14, 2016.

[20] A. Freddi, S. Longhi, A. Monteriù, and D. Ortenzi, "A kinematic joint fault tolerant control based on relative jacobian method for dual arm manipulation systems," in *Proc. 3rd Conf. Control Fault-Tolerant Syst. (SysTol)*, Sep. 2016, pp. 39–44.

[21] J. Zhang, X. Xu, X. Liu, and M. Zhang, "Relative dynamic modeling of dual-arm coordination robot," in *Proc. IEEE Int. Conf. Robot. Biomimetics (ROBIO)*, Dec. 2018, pp. 2045–2050.

[22] Z.-G. Hou, L. Cheng, and M. Tan, "Multicriteria optimization for coordination of redundant robots using a dual neural network," *IEEE Trans. Syst., Man, Cybern., B (Cybern.)*, vol. 40, no. 4, pp. 1075–1087, Aug. 2010.

[23] S. Li, S. Chen, B. Liu, Y. Li, and Y. Liang, "Decentralized kinematic control of a class of collaborative redundant manipulators via recurrent neural networks," *Neurocomputing*, vol. 91, pp. 1–10, Aug. 2012.

[24] L. Jin and Y. Zhang, "G2-type SRMPC scheme for synchronous manipulation of two redundant robot arms," *IEEE Trans. Cybern.*, vol. 45, no. 2, pp. 153–164, Feb. 2015.

[25] D. Chen and Y. Zhang, "Jerk-level synchronous repetitive motion scheme with gradient-type and zeroing-type dynamics algorithms applied to dual-arm redundant robot system control," *Int. J. Syst. Sci.*, vol. 48, no. 13, pp. 2713–2727, Oct. 2017.

[26] Y. Li, S. Li, and B. Hannaford, "A novel recurrent neural network for improving redundant manipulator motion planning completeness," in *Proc. IEEE Int. Conf. Robot. Autom. (ICRA)*, May 2018, pp. 2956–2961.

[27] D. Guo, Z. Li, A. H. Khan, Q. Feng, and J. Cai, "Repetitive motion planning of robotic manipulators with guaranteed precision," *IEEE Trans. Ind. Informat.*, vol. 17, no. 1, pp. 356–366, Jan. 2020.

[28] K. Liu, W.-A. Zhang, H. Dong, and L. Yu, "Trajectory tracking control of three-joint mechanical manipulators based on the disturbance rejection method," in *Proc. 33rd Chin. Control Conf.*, Jul. 2014, pp. 3489–3493.

[29] A. J. Humaidi, H. M. Badr, and A. R. Ajil, "Design of active disturbance rejection control for single-link flexible joint robot manipulator," in *Proc. 22nd Int. Conf. Syst. Theory, Control Comput. (ICSTCC)*, Oct. 2018, pp. 452–457.
[30] W. Deng, J. Yao, and D. Ma, "Time-varying input delay compensation for nonlinear systems with additive disturbance: An output feedback approach," *Int. J. Robust Nonlinear Control*, vol. 28, no. 1, pp. 31–52, Jan. 2018.
[31] C. Zhao, C. Yu, and J. Yao, "Dynamic decoupling based robust synchronous control for a hydraulic parallel manipulator," *IEEE Access*, vol. 7, pp. 30548–30562, 2019.
[32] C. Yang, Y. Jiang, J. Na, Z. Li, L. Cheng, and C.-Y. Su, "Finite-time convergence adaptive fuzzy control for dual-arm robot with unknown kinematics and dynamics," *IEEE Trans. Fuzzy Syst.*, vol. 27, no. 3, pp. 574–588, Mar. 2019.
[33] Z. Dong, J. Ma, and J. Yao, "Barrier function-based asymptotic tracking control of uncertain nonlinear systems with multiple states constraints," *IEEE Access*, vol. 8, pp. 14917–14927, 2020.
[34] W. Deng and J. Yao, "Extended-State-Observer-Based adaptive control of electrohydraulic servomechanisms without velocity measurement," *IEEE/ASME Trans. Mechatronics*, vol. 25, no. 3, pp. 1151–1161, Jun. 2020.
[35] A. Colome and C. Torras, "Closed-loop inverse kinematics for redundant robots: Comparative assessment and two enhancements," *IEEE/ASME Trans. Mechatronics*, vol. 20, no. 2, pp. 944–955, Apr. 2015.
[36] D. Guo, Z. Nie, and L. Yan, "Novel discrete-time zhang neural network for time-varying matrix inversion," *IEEE Trans. Syst., Man, Cybern. Syst.*, vol. 47, no. 8, pp. 2301–2310, Aug. 2017.
[37] D. Guo, F. Xu, Z. Li, Z. Nie, and H. Shao, "Design, verification, and application of new discrete-time recurrent neural network for dynamic nonlinear equations solving," *IEEE Trans. Ind. Informat.*, vol. 14, no. 9, pp. 3936–3945, Sep. 2018.
[38] D. Guo, L. Yan, and Z. Nie, "Design, analysis, and representation of novel five-step DTZD algorithm for time-varying nonlinear optimization," *IEEE Trans. Neural Netw. Learn. Syst.*, vol. 29, no. 9, pp. 4248–4260, Sep. 2018.
[39] *Optim. Toolbox for Use With MATLAB, version 2.3*, The Math Works Inc., Natick, MA, USA, 2003.
[40] J. H. Mathews and K. D. Fink, *Numerical Methods Using MATLAB*, 4th ed. Englewood Cliffs, NJ, USA: Prentice-Hall, 2004.
[41] D. F. Griffiths and D. J. Higham, *Numerical Methods for Ordinary Differential Equations: Initial Value Problems*. London, U.K.: Springer, 2010.
[42] S. Li, L. Jin, and M. A. Mirza, *Kinematic Control of Redundant Robot Arms Using Neural Networks*. Hoboken, NJ, USA: Wiley, 2019.
[43] Z. Yao, J. Yao, and W. Sun, "Adaptive RISE control of hydraulic systems with multilayer neural-networks," *IEEE Trans. Ind. Electron.*, vol. 66, no. 11, pp. 8638–8647, Nov. 2019.
[44] D. Guo, S. Li, and P. S. Stanimirovic, "Analysis and application of modified ZNN design with robustness against harmonic noise," *IEEE Trans. Ind. Informat.*, vol. 16, no. 7, pp. 4627–4638, Jul. 2020.
[45] J. Yao, W. Deng, and W. Sun, "Precision motion control for electro-hydraulic servo systems with noise alleviation: A desired compensation adaptive approach," *IEEE/ASME Trans. Mechatronics*, vol. 22, no. 4, pp. 1859–1868, Aug. 2017.
[46] Z. Zhang, Y. Lin, S. Li, Y. Li, Z. Yu, and Y. Luo, "Tricriteria optimization-coordination motion of Dual-Redundant-Robot manipulators for complex path planning," *IEEE Trans. Control Syst. Technol.*, vol. 26, no. 4, pp. 1345–1357, Jul. 2018.
[47] J. Shao, D. Luo, Y. Xu, and H. Duan, "Cooperative path planning for multiple robots with motion constraints in obstacle-strewn environment," *IEEE Access*, vol. 7, pp. 132286–132301, 2019.

TIE WANG received the B.S. degree from Qiqihar University, Heilongjiang, China, in 2005, and the M.S. degree from Jilin University, Jilin, China, 2010.

He is currently an Associate Researcher with the Logistics Management Department, Qiqihar Medical University. His current research interests include robotics, information processing, and intelligent reform.

DONGSHENG GUO (Member, IEEE) received the B.S. degree in automation from Sun Yat-sen University, Guangzhou, China, in 2010, and the Ph.D. degree in communication and information systems from the School of Information Science and Technology, Sun Yat-sen University, in 2015.

He is currently an Associate Professor with the College of Information Science and Engineering, Huaqiao University, Xiamen, China, and the Fujian Engineering Research Center of Motor Control and System Optimal Schedule, Xiamen, for cooperative research. His current research interests include robotics, neural networks, and numerical methods.